WEATHER CLIMATE WATER

WORLD METEOROLOGICAL ORGANIZATION | GLOBAL ATMOSPHERE WATCH

WMO GREENHOUSE GAS BULLETIN

The State of Greenhouse Gases in the Atmosphere Based on Global Observations through 2023

No. 20 | 28 October 2024

ISSN 2078-0796

The WMO Global Atmosphere Watch (GAW) Greenhouse Gas (GHG) Bulletin has been informing policy and the public on the composition of GHGs in the global atmosphere since 2006. The first edition reported that in 2004, the carbon dioxide (CO_2) level was 377.1 parts per million (ppm[(1)]). In 2023, the level was 420.0 ppm. This is an increase of 42.9 ppm, or 11.4%, in just 20 years.

Atmospheric carbon dioxide (CO_2) is the most important anthropogenic greenhouse gas driving climate change [1]. From 2022 to 2023, the annual mean CO_2 in the global surface atmosphere increased by 2.3 ppm (Figure 1). This increase marked the twelfth consecutive year with an increase greater than 2 ppm, continuing an already significant trend. CO_2 is accumulating in the atmosphere faster than at any time during human existence. The current atmospheric CO_2 level is already 51% above that of the pre-industrial (before 1750) era.

A detailed analysis (Figure 2) of within-year variability demonstrated that the within-year increase of CO_2 in 2023 was 2.8 ppm [3], which is the fourth largest within-year annual increase since modern CO_2 measurements started in the 1950s.

The reason behind this decade-long significant increase in CO_2 is historically large fossil fuel CO_2 emissions in the 2010s and 2020s. It is estimated that global fossil fuel carbon emissions in 2023 were 10.0±0.5 Pg C yr^{-1},

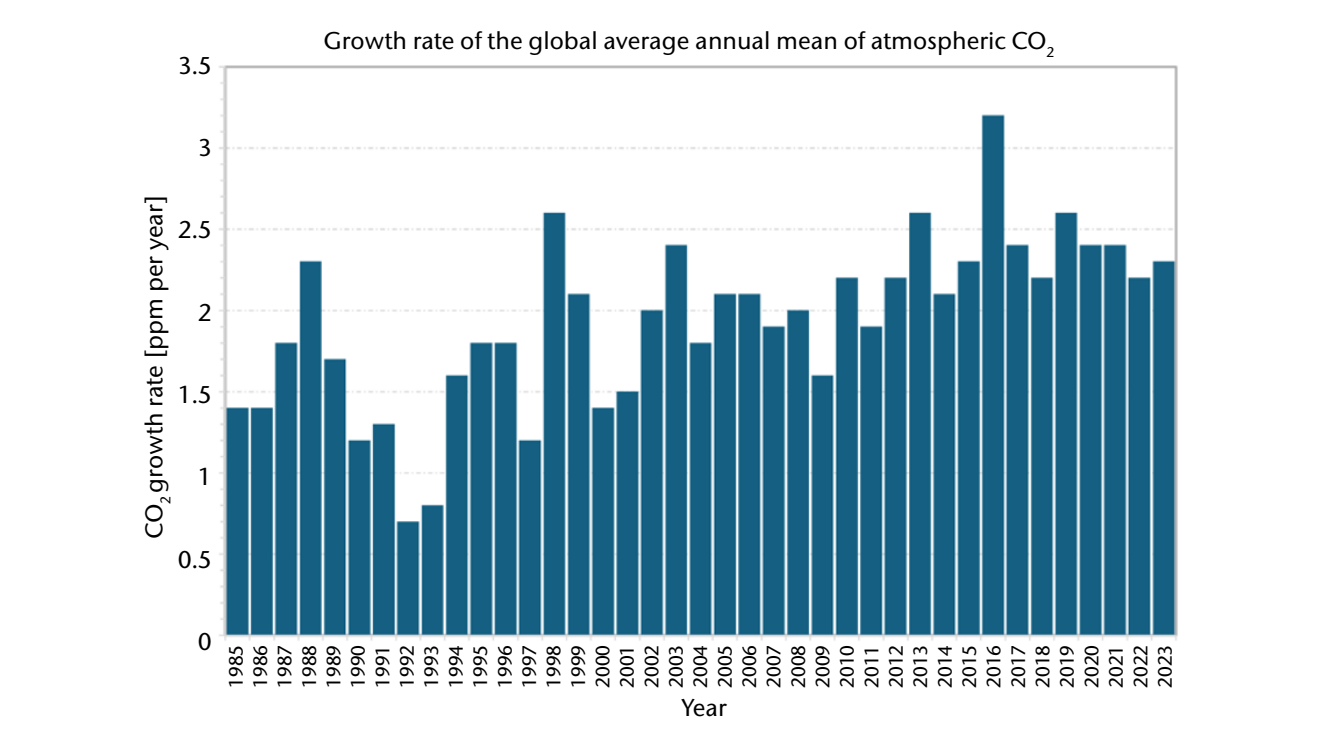

Figure 1. Growth rate of the annual global mean atmospheric CO_2, calculated from WMO GAW network observations for the period 1985–2023 following the method described in [2].

which equals about 37 Pg CO_2 yr^{-1} [4], a significant increase from 3.0±0.2 Pg C yr^{-1} in the 1960s. The increase in atmospheric CO_2 is directly related to the amount of carbon emissions because it is the net result of total carbon emissions surpassing total ocean and terrestrial biosphere carbon sinks. Although the growth rate of fossil fuel carbon emissions has slowed in the recent decade compared to the 2000s, fossil fuel carbon emissions remain high. This has resulted in the largest decadal average growth in atmospheric CO_2 in the record, 2.4 ppm yr^{-1}, between 2014 and 2023.

In 2023, the within-year increase of atmospheric CO_2 was larger than the decadal average and was the second largest within-year growth in the past decade. This may be a result of enhanced fire emissions and reduced net terrestrial carbon sinks. While the long-term CO_2 increase caused by fossil fuel combustion is monotonic, the CO_2 growth rate varies from year to year (ranging from 2.1 ppm to 3.2 ppm from 2014 to 2023 (Figure1)), with the variability mostly driven by the terrestrial biosphere exchange of CO_2, as confirmed by measurements of the stable carbon isotopic ratio, ^{13}C:^{12}C, in atmospheric CO_2 [5, 6]. The El Niño–Southern Oscillation (ENSO) is the main driver of this interannual variability [7, 8], which impacts photosynthetic CO_2 uptake, respiratory release, and fires. In May 2023, the Earth transitioned from a three-year-long La Niña to an El Niño, that is, from the cold phase to the warm phase of ENSO, which also caused a record-high global average temperature.

Coincidental with the large CO_2 increase during 2023 (Figure 2) was the largest increase in atmospheric carbon monoxide (CO) in the past two decades [9], suggesting enhanced CO_2 emissions from fires. Carbon monoxide results from incomplete combustion, and enhanced CO levels from background locations away from traffic and industrial emissions is a good indicator of fire emissions. In 2023, Canada experienced its worst wildfire season on record, emitting 0.65 Pg C, comparable to the annual fossil fuel carbon emissions from some large nations [10]. From August to October, Australia experienced its driest three-month period on record, with severe bushfires [11]. Global fire carbon emissions were 2.4 Pg C, 16% above average, during the 2023–2024 global fire season, which ranks seventh among all fire seasons since 2003 [12]. It is estimated that the net ecosystem carbon exchange, another important part of the land CO_2 flux, was approximately 28% lower in 2023 than in 2021–2022, based on an atmospheric tracer transport model which optimizes CO_2 flux by using atmospheric CO_2 measurements [13]. 2023 was an exceptionally warm year; global temperature across the land and the oceans was the highest in records dating as far back as 1850 [11]. Extreme heat is a stress factor for many terrestrial systems and can cause reduced carbon uptake by plants. Research is still ongoing to better estimate the exact source and sink attributions for the large CO_2 increase during 2023.

In the near future, climate change feedbacks could cause ecosystems to become larger sources (see, for example [14]) or sinks of GHGs. Wildfires could release more CO_2 into the atmosphere and the warmer oceans could absorb less CO_2. As a consequence, more CO_2 could stay in the atmosphere, accelerating global warming and ocean acidification. These climate feedbacks are critical concerns to societies worldwide.

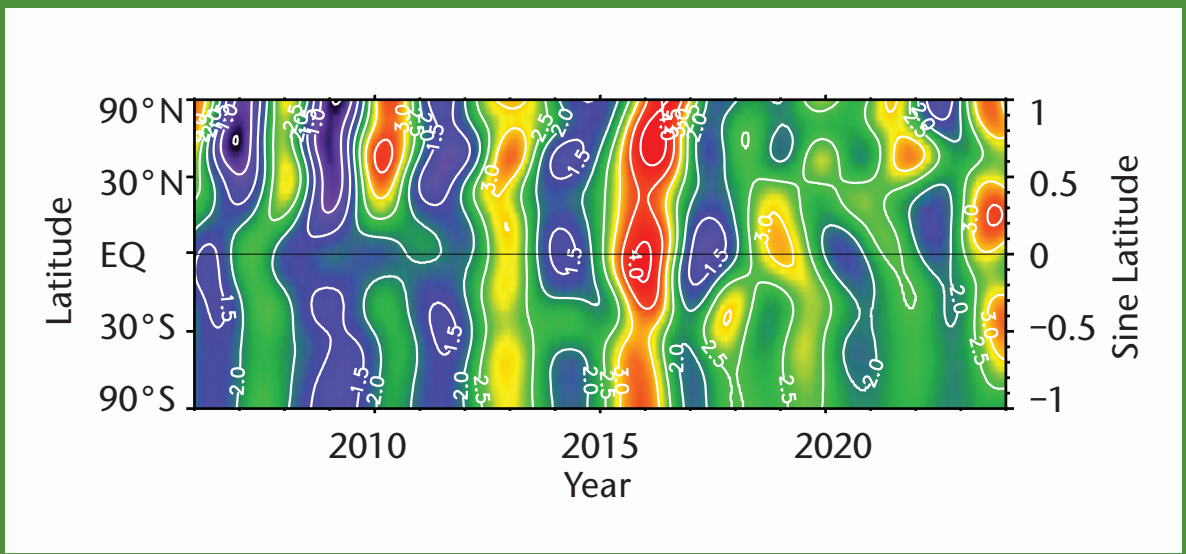

Figure 2. Growth rate contour of atmospheric CO_2 determined from National Oceanic and Atmospheric Administration (NOAA) Global Monitoring Laboratory (GML) measurements at marine boundary layer sites that represent a large volume of atmosphere. The contours indicate the CO_2 growth rate in ppm yr^{-1}. The colder colours indicate relatively smaller (though still historically high) growth rates, and the warmer colours indicate relatively larger growth rates.

Executive summary

The latest analysis of observations from the WMO Global Atmosphere Watch (GAW) in situ observational network shows that the globally averaged surface concentrations[2] for carbon dioxide (CO_2), methane (CH_4) and nitrous oxide (N_2O) reached new highs in 2023, with CO_2 at 420.0±0.1 ppm, CH_4 at 1934±2 ppb[3] and N_2O at 336.9±0.1 ppb. These values constitute, respectively, increases of 151%, 265% and 125% relative to pre-industrial (before 1750) levels. The increase in CO_2 from 2022 to 2023 was slightly higher than the increase observed from 2021 to 2022 and slightly lower than the average annual growth rate over the last decade, and was most likely partly caused by natural variability, as fossil fuel CO_2 emissions have continued to increase. For CH_4, the increase from 2022 to 2023 was lower than that observed from 2021 to 2022 but still slightly higher than the average annual growth rate over the last decade. For N_2O, the increase from 2022 to 2023 was lower than that observed from 2021 to 2022, which was the highest increase observed in our modern time record. The National Oceanic and Atmospheric Administration (NOAA) Annual Greenhouse Gas Index (AGGI) [15] shows that from 1990 to 2023, radiative forcing by long-lived greenhouse gases (LLGHGs) increased by 51.5%, with CO_2 accounting for about 81% of this increase.

Overview of observations from the GAW in situ observational network for 2023

This twentieth annual WMO Greenhouse Gas Bulletin reports atmospheric abundances and rates of change of the most important long lived greenhouse gases (LLGHGs) – carbon dioxide, methane, and nitrous oxide – and provides a summary of the contributions of other greenhouse gases. CO_2, CH_4 and N_2O, together with dichlorodifluoromethane (CFC-12) and trichlorofluoromethane (CFC-11), account for approximately 96%[4] [15] of radiative forcing due to LLGHGs (Figure 3).

Table. Global annual surface mean abundances (2023) and trends of key greenhouse gases from the GAW in situ observational network for GHG. Units are concentrations in dry-air, and uncertainties are 68% confidence limits. The averaging method is described in GAW Report No. 184 [2].

	CO_2	CH_4	N_2O
2023 global mean abundance	420.0±0.1 ppm	1934±2 ppb	336.9±0.1 ppb
2023 abundance relative to 1750[a]	151%	265%	125%
2022–2023 absolute increase	2.3 ppm	11 ppb	1.1 ppb
2022–2023 relative increase	0.55%	0.57%	0.33%
Mean annual absolute increase over the past 10 years	2.4 ppm yr^{-1}	10.7 ppb yr^{-1}	1.07 ppb yr^{-1}

[a] Assuming a pre-industrial concentration of 278.3 ppm for CO_2, 729.2 ppb for CH_4 and 270.1 ppb for N_2O. The number of stations used for the analyses was 146 for CO_2, 153 for CH_4 and 112 for N_2O.

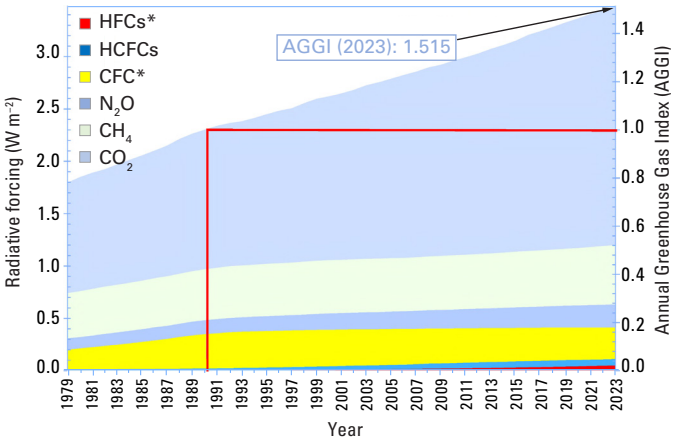

Figure 3. Atmospheric radiative forcing relative to 1990 by LLGHGs corresponding to the 2023 update of the NOAA AGGI [15]. The "CFC*" grouping includes some other long-lived gases that are not CFCs (e.g., CCl_4, CH_3CCl_3, and Halons), but the CFCs account for the majority (95% in 2023) of this radiative forcing. The "HCFC" grouping includes the three most abundant of these chemicals (HCFC-22, HCFC-141b, and HCFC-142b). The "HFC*" grouping includes the most abundant HFCs (HFC-134a, HFC-23, HFC-125, HFC-143a, HFC-365mfc, HFC-227ea and HFC-152a) and SF_6 for completeness, although SF_6 only accounted for a small fraction of the radiative forcing from this group in 2023 (13%).

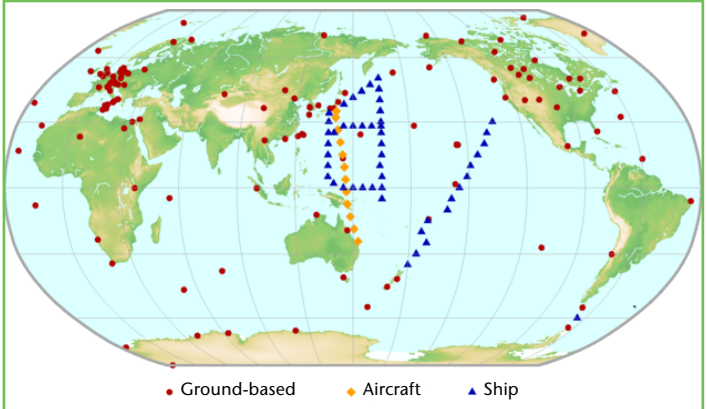

Figure 4. The GAW global network for CO_2 in the last decade. The network for CH_4 is similar. The in situ network for N_2O and other LLGHGs is far less dense.

The WMO Global Atmosphere Watch Programme coordinates systematic observations and analyses of GHGs and other trace species. Sites where greenhouse gases have been measured in the last decade are shown in Figure 4. Measurement data are reported by participating countries and archived and distributed by the World Data Centre for Greenhouse Gases (WDCGG) at the Japan Meteorological Agency.

The results reported here by WMO WDCGG for the global average and growth rate are slightly different from the results reported by NOAA for the same years [3] due to differences in the stations used and the averaging

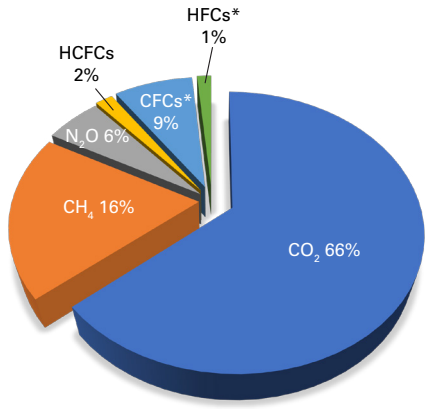

Figure 5. Contribution of the most important long-lived greenhouse gases to the increase in global radiative forcing from the pre-industrial era to 2023 [15]

procedure, as well as a slight difference in the time period for which the numbers are representative. WMO WDCGG follows the procedure described in detail in GAW Report No. 184 [2].

The table provides globally averaged atmospheric abundances of the three major LLGHGs in 2023 and changes in their abundances since 2022 and 1750.

The three GHGs shown in the table are closely linked to anthropogenic activities and interact strongly with the biosphere and the oceans. Predicting the evolution of the atmospheric content of GHGs requires a quantitative understanding of their many sources, sinks and chemical transformations in the atmosphere. Observations from GAW provide invaluable constraints on the budgets of these and other LLGHGs and are used to improve emission estimates and evaluate satellite retrievals of LLGHG column averages. The Integrated Global Greenhouse Gas Information System (IG^{3}IS) provides further insights on the sources of GHGs at the national and sub-national, especially urban, scales.

The NOAA AGGI measures the increase in total radiative forcing due to all LLGHGs since 1990 [15]. The AGGI reached 1.51 in 2023, representing a 51.5% increase in total radiative forcing[4] from 1990 to 2023 and a 1.6% increase from 2022 to 2023 (Figure 3). The relative contributions of other gases in the total radiative forcing since the pre-industrial era are presented in Figure 5.

Carbon dioxide (CO_2)

Carbon dioxide is the single most important anthropogenic greenhouse gas in the atmosphere, accounting for approximately 66%[4] of the radiative forcing by LLGHGs. It is responsible for about 79%[4] of the increase in radiative forcing over the past decade and about 77% of the increase over the past five years. The pre-industrial level of 278.3 ppm represented a balance of fluxes among the atmosphere, the oceans and the land biosphere. The globally averaged CO_2 concentration in 2023 was 420.0±0.1 ppm (Figure 6a). The increase in the annual mean from 2022 to 2023, 2.3 ppm, was slightly higher than the 2.2 ppm increase from 2021 to 2022 and only slightly lower than the average growth rate for the past decade (2.4 ppm yr^{-1}). The slight decrease in growth rates does not point to decreasing fossil fuel emissions, as discussed in the cover story, but rather relates to natural variability. The observed growth rate is a result of continued high fossil fuel emissions, increased emissions from fires and possibly a reduced land sink in 2023. The scientific consensus is that variability in the atmospheric CO_2 growth rate (Figure 6b) arises mainly from changing amounts of net CO_2 absorption by terrestrial ecosystems.

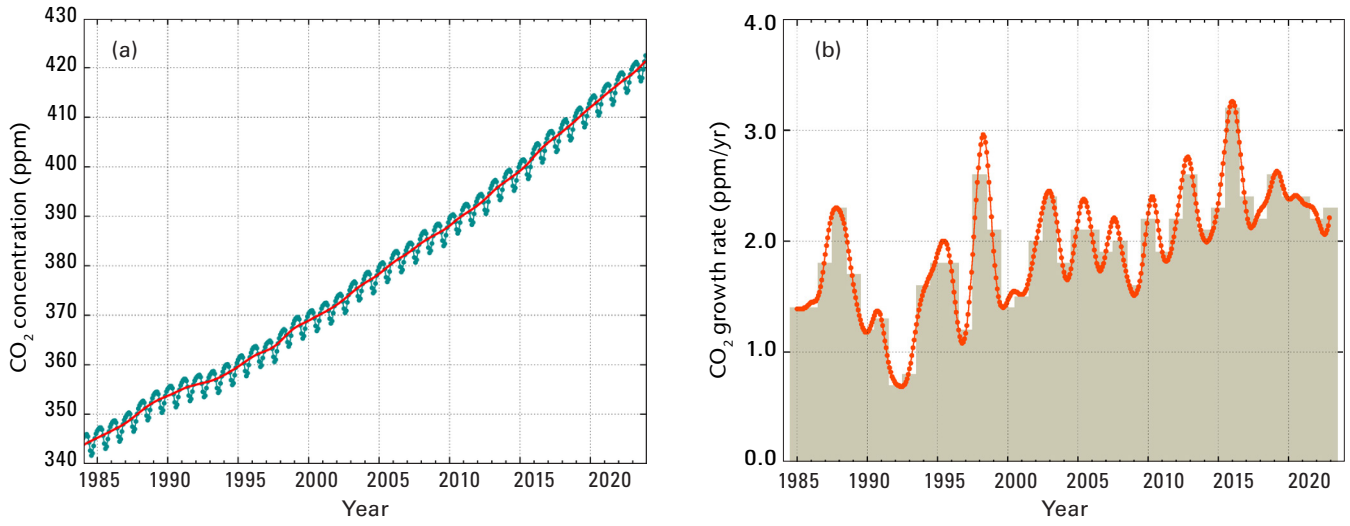

Figure 6. Globally averaged CO_2 concentration (a) and its growth rate (b) from 1984 to 2023. Increases in successive annual means are shown as the shaded columns in (b). The red line in (a) is the monthly mean with the seasonal variation removed; the blue dots and blue line in (a) depict the monthly averages. Observations from 146 stations were used for this analysis.

Rapid increase in atmospheric CH_4 and decrease in $\delta^{13}C_{CH4}$ from 2020 to 2022 suggest a dominant microbial emission increase

Concerns about climate feedback are not limited to carbon dioxide (CO_2). From 2020 to 2022, atmospheric methane (CH_4) experienced its largest three-year increase, 15.4 ppb yr^{-1}, since systematic global CH_4 measurements began in the 1980s. Observations and model simulations point to a significant increase in CH_4 emissions from natural wetlands in response to warmer temperatures and particularly wetter land conditions during the 2020–2022 La Niña.

Atmospheric CH_4 is the second largest contributor to increased climate forcing. It is emitted from anthropogenic sources, such as fossil fuel exploitation, livestock, waste and landfills, and rice cultivation, and natural sources, such as wetlands and shallow lakes. Atmospheric CH_4 is removed by reactions with various oxidants in the atmosphere and consumed by soil microbes. Methane emitted from different sources carries distinct fingerprints in its stable carbon isotopes, ^{13}C:^{12}C (denoted as $\delta^{13}C_{CH4}$), which serve as unique signatures for CH_4 emissions (see WMO Greenhouse Gas Bulletin No. 15). Different CH_4 removal mechanisms also affect $\delta^{13}C_{CH4}$ in the atmosphere. Atmospheric $\delta^{13}C_{CH4}$ measurements are used to further understand CH_4 emissions from different source sectors (see Figure 10 for a detailed approach).

Atmospheric CH_4 levels have increased significantly since the beginning of the industrial era, from 729±9 ppb in the pre-industrial period [20] to 1774±2 ppb in the 1999–2006 period, when the increase temporarily paused. From 1800 to the early 2000s, the amount of $\delta^{13}C_{CH4}$ in the atmosphere also increased significantly [21], indicating a long-term CH_4 increase in ^{13}C-enriched fossil fuel emissions. Atmospheric CH_4 began increasing again in 2007; this increase accelerated in 2014 and further accelerated in 2020. Around the same time that the 2007 CH_4 increase began, atmospheric $\delta^{13}C_{CH4}$ started to decrease. The record rise in atmospheric CH_4 from 2020 to 2022 was accompanied by a significant drop in atmospheric $\delta^{13}C_{CH4}$ (Figure 11). The unexpected change in the amount of atmospheric $\delta^{13}C_{CH4}$ is best explained by a transition from fossil fuels to microbial emissions as the dominant driver of increasing CH_4 because microbial CH_4 emissions are generally more depleted in $\delta^{13}C_{CH4}$ than atmospheric $\delta^{13}C_{CH4}$ (Figure 10). Increased fossil fuel emissions since 2007 have contributed to a small fraction, about 15%, of the global increase in CH_4 emissions [22]. Several global CH_4 transport models that assimilate atmospheric CH_4 and $\delta^{13}C_{CH4}$ measurements have consistently identified increased microbial emissions as the primary driver of recent increases in atmospheric CH_4. The geographic distribution of CH_4 growth and

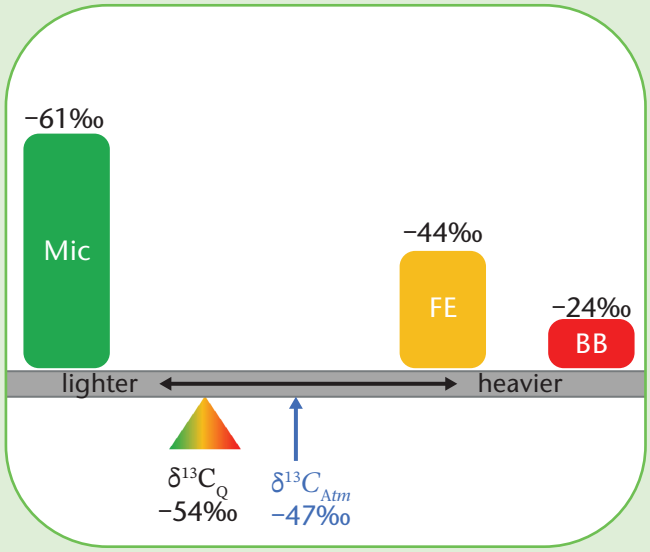

Figure 10. See-saw illustrations of the $\delta^{13}C_{CH4}$ mass balance constraint on source partitioning (lighter $\delta^{13}C_{CH4}$ to the left and heavier to the right). The total source signature ($\delta^{13}C_Q$) is balanced by different CH_4 emissions from microbials (Mic), fossil (FE), and biomass/biofuel burning (BB) sources with their global mean $\delta^{13}C_{CH4}$ signatures in ‰. Mic sources such as wetlands, livestock, waste and rice paddies are generally the lightest (lowest $\delta^{13}C$), and pyrogenic sources such as wildfires and biofuels generally the heaviest (highest $\delta^{13}C$), with fossil sources in between. The difference between total source signature ($\delta^{13}C_Q$) and atmospheric $\delta^{13}C_{CH4}$ is the total sink signature. If the total sink signature is known, atmospheric $\delta^{13}C_{CH4}$ can be used to find the horizontal position of the total emission signature ($\delta^{13}C_Q$). Then the sizes of individual emissions must balance the left see-saw. Note that approximate values are shown in this figure.

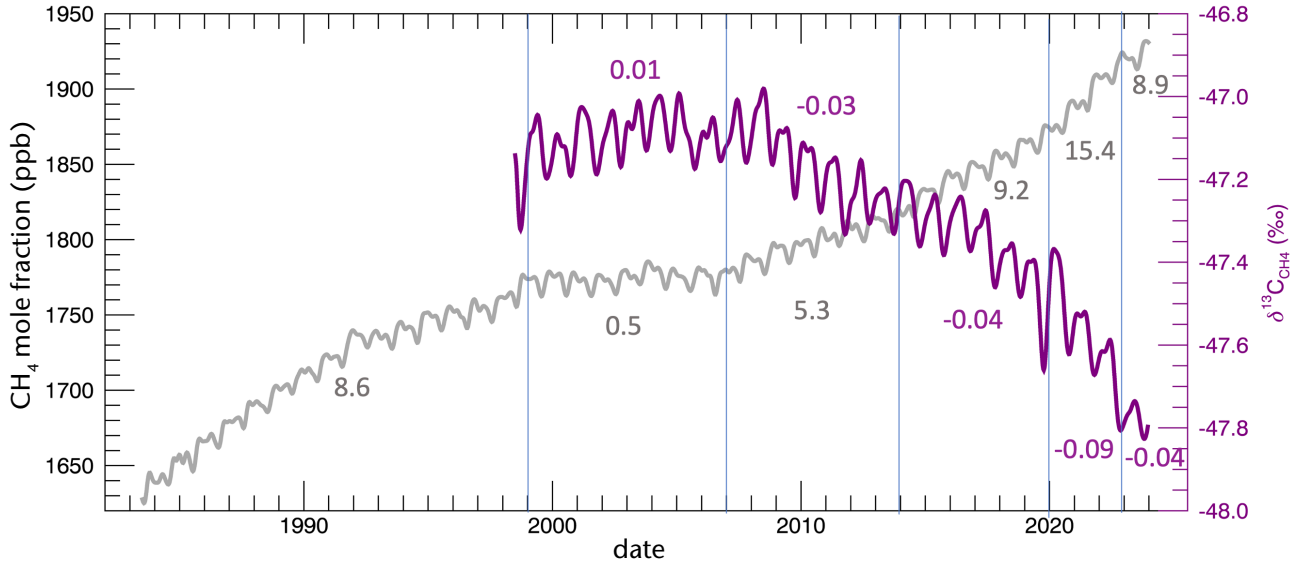

Figure 11. Globally-averaged CH_4 abundance (in gray) and $\delta^{13}C_{CH4}$ (purple) from NOAA Global Monitoring Laboratory and the Institute of Arctic and Alpine Research. Mean growth rates are shown in text for CH_4 and $\delta^{13}C_{CH4}$ (in ppb yr^{-1} and ‰ yr^{-1}, respectively) for the following time periods: 1983-1998, 1999-2006, 2008-2013, 2014-2019, 2020-2022 and 2023.

the rapid drop in atmospheric $\delta^{13}C_{CH4}$ from 2020 to 2022 suggest strong increases in isotopically light (biogenic) emissions, which, in combination with the other studies [23, 24, 25, 26], may indicate a positive climate feedback with respect to CH_4 emissions. In 2023, the global climate transitioned to an El Niño phase, and a slowdown was observed in the increase in global CH_4 compared to the 2020–2022 period, with the within-year increase at 8.9 ppb yr^{-1}, accompanied by a slowdown in the decrease in $\delta^{13}C_{CH4}$; these changes could be the result of increased biomass burning emissions (heavy in $\delta^{13}C_{CH4}$) and reduced wetland CH_4 emissions due to warmer and drier conditions in 2023.

Another potential climate feedback is the thawing of the Arctic permafrost, which can release organic carbon, which microbes then convert to CO_2 and CH_4. However, a large increase in carbon emissions from the Arctic has not (yet) been detected. A relatively small amount of permafrost CH_4 emissions may have contributed to the small increase in recent Arctic microbial CH_4 emissions [27]. Arctic landmasses hold huge stores of carbon, on the order of 1 000 Pg C, in the top three meters of permafrost [28]. For comparison, the current atmosphere holds 4 Pg C as CH_4. Such climate feedback would be extremely difficult to control.

The best approach for humanity is to stop feeding a future climate scenario with significant climate feedback by reducing current greenhouse gas emissions, especially CO_2 [29]. To support effective emissions reduction policies, greenhouse gases need to be monitored in such a way that the measurements can provide objective and authoritative quantification of emissions and removals. These measurements must be precise and well-calibrated, because the information about emissions resides in small gradients in space and time relative to a common global background. They must also be sustained over decades to track progress on climate action. Satellite retrievals can supplement this effort, especially for regions where it is difficult to have precise and well-calibrated greenhouse gas measurements.

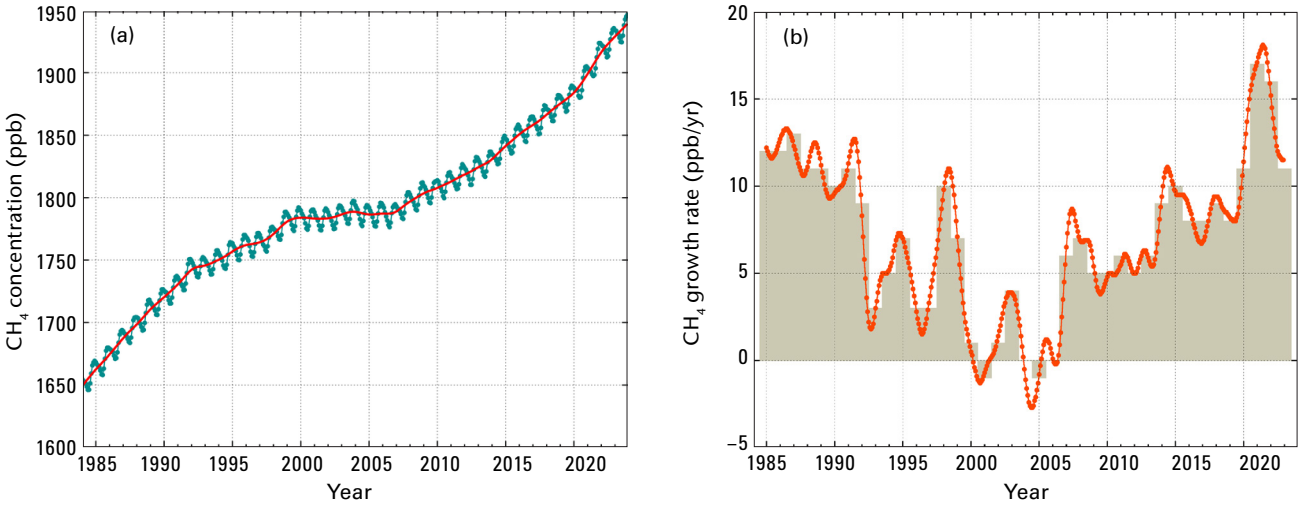

Figure 7. Globally averaged CH_4 concentration (a) and its growth rate (b) from 1984 to 2023. Increases in successive annual means are shown as the shaded columns in (b). The red line in (a) is the monthly mean with the seasonal variation removed; the blue dots and blue line in (a) depict the monthly averages. Observations from 153 stations were used for this analysis.

Atmospheric CO_2 reached 151% of the pre-industrial level in 2023, primarily because of emissions from the combustion of fossil fuels and cement production. According to the International Energy Agency (IEA), fossil fuel CO_2 emissions were projected to be 37.4 billion tonnes (Pg or Gt[5]) of CO_2 in 2023, up 1.1% from 37 Gt CO_2 in 2022 [16]. According to the 2023 analysis of the Global Carbon Project, deforestation and other land-use change averaged 4.7 (±2.6) Gt CO_2 yr^{-1} for the 2013–2022 period. Of the total emissions from human activities during the 2013–2022 period, about 43% accumulated in the atmosphere, 26% in the ocean and 31% on land, with the unattributed budget imbalance being just under 1% [4]. The portion of CO_2 emitted by fossil fuel combustion that remains in the atmosphere (the airborne fraction, (AF)), varies inter-annually due to the high natural variability of (mainly terrestrial) CO_2 sinks, although there is little evidence for a long-term AF trend (see the cover story in WMO Greenhouse Gas Bulletin No. 17).

Methane (CH_4)

Methane accounts for about 16%[4] of the radiative forcing by LLGHGs. Approximately 40% of methane is emitted into the atmosphere by natural sources (for example, wetlands and termites), and about 60% comes from anthropogenic sources (for example, ruminants, rice agriculture, fossil fuel exploitation, landfills, wastewater and biomass burning) [17]. The globally averaged CH_4 concentration calculated from in situ observations reached a new high of 1934±2 ppb in 2023, an increase of 11 ppb with respect to the previous year (Figure 7a). This increase was lower than the increase of 16 ppb from 2021 to 2022 and slightly higher than the average annual increase of 10.7 ppb over the past decade. The mean annual increase of CH_4 decreased from approximately 12 ppb yr^{-1} during the late 1980s to near zero during 1999–2006 (Figure 7b). Since 2007, atmospheric CH_4 has been increasing. It reached 265% of the pre-industrial level in 2023, driven by increased emissions from anthropogenic sources. It is critical to remember that unlike the case with CO_2, CH_4 anthropogenic sources are not dominated by fossil fuel-related emissions; agricultural sources also play an important role. Studies using GAW CH_4 measurements indicate that increased CH_4 emissions from wetlands in the tropics and from anthropogenic sources at the mid-latitudes of the northern hemisphere are the likely causes of this recent increase (see insert).

Nitrous Oxide (N_2O)

Nitrous oxide accounts for about 6%[4] of the radiative forcing by LLGHGs. It is the third most important individual contributor to the combined forcing. N_2O is emitted into the atmosphere from both natural sources (approximately 57%) and anthropogenic sources (approximately 43%), including oceans, soils, biomass burning, fertilizer use, and various industrial processes. The globally averaged N_2O concentration in 2023 reached 336.9±0.1 ppb, which is an increase of 1.1 ppb with respect to the previous year (Figures 8a and 8b) and 125% of the pre-industrial level (270.1 ppb). The annual increase from 2022 to 2023 was lower than the increase from 2021 to 2022 and slightly higher than the mean growth rate over the past 10 years (1.07 ppb yr^{-1}). Global human-induced N_2O emissions, which are dominated by nitrogen additions to croplands, increased by 30% over the past four decades to 7.3 (range: 4.2–11.4) teragrams of nitrogen per year. This increase was mainly responsible for the growth in the atmospheric burden of N_2O [18].

Other greenhouse gases

Stratospheric ozone-depleting CFCs, which are regulated by the Montreal Protocol on Substances that Deplete the Ozone Layer, together with minor halogenated

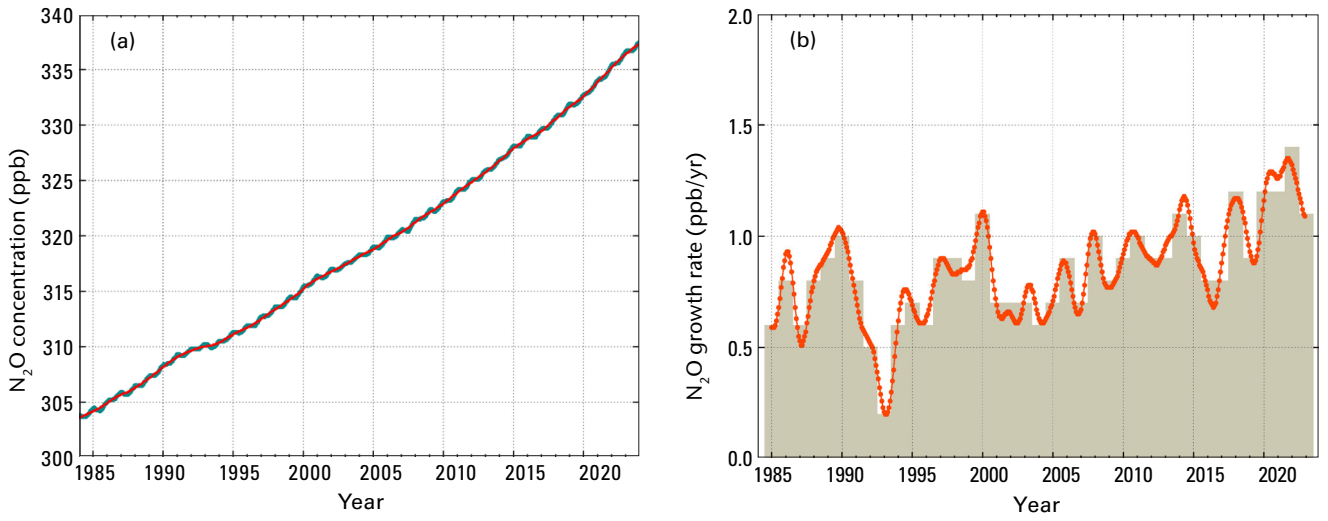

Figure 8. Globally averaged N_2O concentration (a) and its growth rate (b) from 1984 to 2023. Increases in successive annual means are shown as the shaded columns in (b). The red line in (a) is the monthly mean with the seasonal variation removed; in this plot, the red line overlaps the blue dots and blue line that depict the monthly averages. Observations from 112 stations were used for this analysis.

gases, account for approximately 12%[4] of the radiative forcing by LLGHGs. While CFCs and most halons are decreasing, some HCFCs and HFCs, which are also potent greenhouse gases, are increasing at relatively rapid rates; however, they are still low in abundance (at ppt[6] levels). Although at a similarly low abundance, SF_6 is an extremely potent LLGHG. It is produced by the chemical industry, mainly as an electrical insulator in power distribution equipment. Its concentration is rising at a quite constant rate and is now more than twice the level observed in the mid-1990s (Figure 9a).

This Bulletin primarily addresses long-lived greenhouse gases. Relatively short-lived tropospheric ozone has a radiative forcing comparable to that of the halocarbons [19]; because of its short lifetime, its horizontal and vertical variability is very high and global means are not well characterized with a network such as that shown in Figure 4. Many other pollutants, such as carbon monoxide, nitrogen oxides and volatile organic compounds, although not referred to as greenhouse gases, have small direct or indirect effect on radiative forcing. Aerosols (suspended particulate matter) are short-lived substances that alter the radiation budget. All the gases mentioned in this Bulletin, as well as aerosols, are included in the observational programme of GAW, with support from WMO Member countries and contributing networks.

Acknowledgements and links

Fifty-five WMO Members contributed CO_2 and other greenhouse gas data to the GAW WDCGG. Approximately 46% of the measurement records submitted to WDCGG were obtained at sites of the NOAA Global Monitoring Laboratory cooperative air-sampling network. For information about the GAW GHG network and methodologies, see GAW Report No. 292. The Advanced

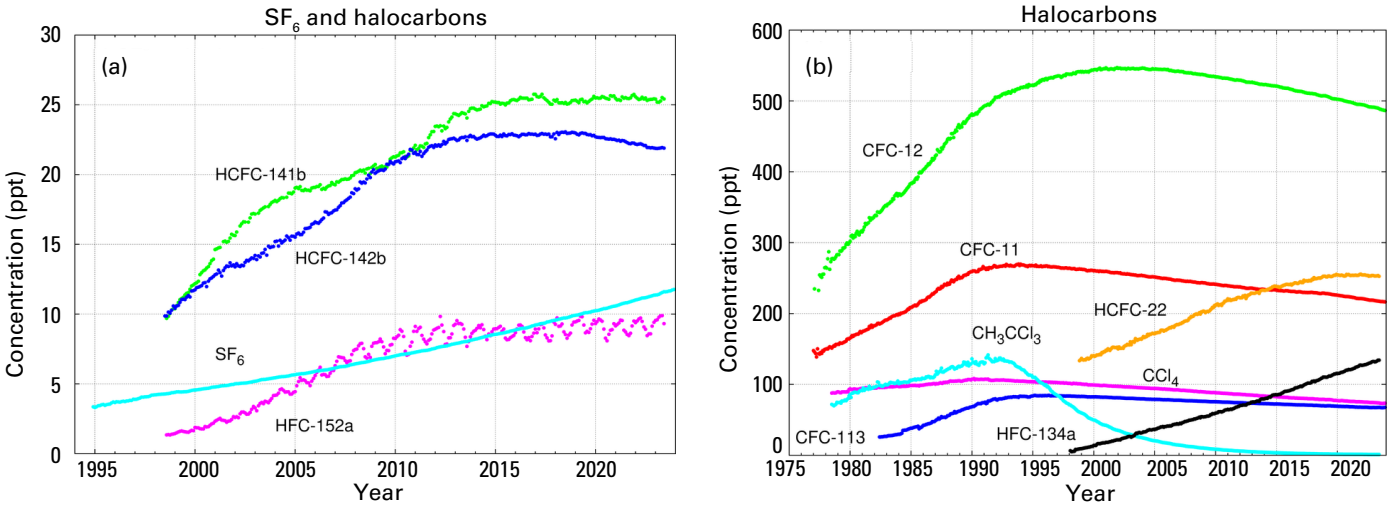

Figure 9. Monthly mean concentration of sulfur hexafluoride (SF_6) and the most important halocarbons: (a) SF_6 and lower mole fractions of halocarbons and (b) higher halocarbon concentration. For each gas, the number of stations used for the analysis was as follows: SF_6 (91), CFC-11 (26), CFC-12 (28), CFC-113 (23), CCl_4 (24), CH_3CCl_3 (26), HCFC-141b (12), HCFC-142b (16), HCFC-22 (16), HFC-134a (12), HFC-152a (12).

Global Atmospheric Gases Experiment also contributed observations to this Bulletin. The GAW observational stations that contributed data to this Bulletin, shown in Figure 4, are included in the list of contributors on the WDCGG web page. They are also described in the GAW Station Information System (GAWSIS), supported by MeteoSwiss, Switzerland. The present Bulletin has been prepared under the oversight of the GAW Scientific Advisory Group on Greenhouse Gases.

Editorial team

Alex Vermeulen, Xin Lan, Oksana Tarasova, Kazuhiro Tsuboi

Authors (in alphabetical order)

Andrew Crotwell (NOAA Global Monitoring Laboratory and Cooperative Institute for Research in Environmental Sciences, University of Colorado Boulder, United States of America), Christoph Gerbig (Max Planck Institute for Biogeochemistry, Germany), Armin Jordan (Max Planck Institute for Biogeochemistry, Germany), Xin Lan (NOAA Global Monitoring Laboratory and Cooperative Institute for Research in Environmental Sciences, University of Colorado Boulder, USA), Zoë Loh (Commonwealth Scientific and Industrial Research Organisation, Australia), Ingrid Luijkx (Wageningen University and Research, Netherlands (Kingdom of the)), John Miller (NOAA Global Monitoring Laboratory, USA), Oksana Tarasova (WMO), Kazuhiro Tsuboi (Japan Meteorological Agency, WDCGG, Japan), Alex Vermeulen (Integrated Carbon Observation System – European Research Infrastructure Consortium (ICOS ERIC)/Lund University, Sweden), Ray Weiss (Scripps Institution of Oceanography, University of California San Diego, USA), Thorsten Warneke (University Bremen, Germany), Camille Yver (Laboratoire des Sciences du Climat et de l'Environnement (LSCE), France)

References

[1] Intergovernmental Panel on Climate Change (IPCC). Climate Change 2022: *Impacts, Adaptation, and Vulnerability. Contribution of Working Group II to the Sixth Assessment Report of the Intergovernmental Panel on Climate Change*; Pörtner, H.-O.; Roberts, D. C.; Tignor, M. et al., Eds.; Cambridge University Press: Cambridge, UK and New York, USA, 2022. https://doi.org/10.1017/9781009325844.

[2] Tsutsumi, Y.; Mori, K.; Hirahara, T. et al. Technical Report of Global Analysis Method for Major Greenhouse Gases by the World Data Center for Greenhouse Gases (WMO/TD-No. 1473). GAW Report No. 184; World Meteorological Organization (WMO): Geneva, 2009.

[3] Lan, X.; Tans, P.; Thoning, K. W.: *Trends in Globally-averaged CO_2 Determined from NOAA Global Monitoring Laboratory Measurements*. Version 2024-10. National Oceanic and Atmospheric Administration (NOAA) Global Monitoring Laboratory, 2024. https://doi.org/10.15138/9N0H-ZH07.

[4] Friedlingstein, P.; O'Sullivan, M.; Jones, M. W. et al. Global Carbon Budget 2023. *Earth System Science Data* **2023**, *15* (12), 5301–5369. https://doi.org/10.5194/essd-15-5301-2023.

[5] Alden, C. B.; Miller, J. B.; White, J. W. C. Can Bottom-up Ocean CO_2 Fluxes Be Reconciled with Atmospheric ^{13}C Observations? *Tellus B: Chemical and Physical Meteorology* **2010**, *62* (5). https://doi.org/10.1111/j.1600-0889.2010.00481.x.

[6] Keeling, C. D.; Revelle, R. Effects of El Nino/Southern Oscillation on the Atmospheric Content of Carbon Dioxide. *Meteoritics* **1985**, *20*, 437–450.

[7] Betts, R. A.; Jones, C. D.; Knight, J. R. et al. El Niño and a Record CO_2 Rise. *Nature Climate Change* **2016**, *6* (9), 806–810. https://doi.org/10.1038/nclimate3063.

[8] Liu, J.; Bowman, K. W.; Schimel, D. S. et al. Contrasting Carbon Cycle Responses of the Tropical Continents to the 2015–2016 El Niño. *Science* **2017**, *358* (6360), eaam5690. https://doi.org/10.1126/science.aam5690.

[9] National Oceanic and Atmospheric Administration (NOAA) Global Monitoring Laboratory, *GGGRN Data – CO*. 2024. https://gml.noaa.gov/ccgg/data/getdata.php?gas=co, accessed on 16 October 2024.

[10] Byrne, B.; Liu, J.; Bowman, K. W. et al. Carbon Emissions from the 2023 Canadian Wildfires. *Nature* **2024**, *633* (8031), 835–839. https://doi.org/10.1038/s41586-024-07878-z.

[11] Blunden, J. and T. Boyer, Eds.: "State of the Climate in 2023". *Bulletin of the American Meteorological Society* **2024**, *105* (8) [special supplement]. https://doi.org/10.1175/2024BAMSStateoftheClimate.1.

[12] Jones, M. W.; Kelley, D. I.; Burton, C. A. et al. State of Wildfires 2023–2024. *Earth System Science Data* **2024**, *16* (8), 3601–3685. https://doi.org/10.5194/essd-16-3601-2024.

[13] Jacobson, A. R., Schuldt, K. N., Tans, P. et al. *CarbonTracker CT2022*. National Oceanic and Atmospheric Administration (NOAA) Global Monitoring Laboratory, 2023. https://doi.org/10.25925/Z1GJ-3254.

[14] Gatti, L. V.; Basso, L. S.; Miller, J. B. et al. Amazonia as a Carbon Source Linked to Deforestation and Climate Change. *Nature* **2021**, *595* (7867), 388–393. https://doi.org/10.1038/s41586-021-03629-6.

[15] Montzka, S. A. *The NOAA Annual Greenhouse Gas Index (AGGI)*; National Oceanic and Atmospheric Administration (NOAA) Earth System Research Laboratories Global Monitoring Laboratory, 2024. http://www.esrl.noaa.gov/gmd/aggi/aggi.html.

[16] International Energy Agency (IEA). *CO_2 Emissions in 2023*; IEA: Paris, 2024. https://www.iea.org/reports/co2-emissions-in-2023.
[17] Saunois, M.; Stavert, A. R.; Poulter, B. et al. The Global Methane Budget 2000–2017. *Earth System Science Data* **2020**, *12* (3), 1561–1623. https://doi.org/10.5194/essd-12-1561-2020.
[18] Tian, H.; Xu, R.; Canadell, J. G. et al. A Comprehensive Quantification of Global Nitrous Oxide Sources and Sinks. *Nature* **2020**, *586* (7828), 248–256. https://doi.org/10.1038/s41586-020-2780-0.
[19] Forster, P.; Storelvmo, T.; Armour, K. et al. The Earth's Energy Budget, Climate Feedbacks, and Climate Sensitivity. In *Climate Change 2021: The Physical Science Basis. Contribution of Working Group I to the Sixth Assessment Report of the Intergovernmental Panel on Climate Change*; Masson-Delmotte, V.; Zhai, P.; Pirani, A. et al., Eds.; Cambridge University Press: Cambridge, UK and New York, USA, 2021. https://www.ipcc.ch/report/ar6/wg1/downloads/report/IPCC_AR6_WGI_Chapter07.pdf.
[20] Mitchell, L.; Brook, E.; Lee, J. E. et al. Constraints on the Late Holocene Anthropogenic Contribution to the Atmospheric Methane Budget. *Science* **2013**, *342* (6161), 964–966. https://doi.org/10.1126/science.1238920.
[21] Ferretti, D. F.; Miller, J. B.; White, J. W. C. et al. Unexpected Changes to the Global Methane Budget over the Past 2000 Years. *Science* **2005**, *309* (5741), 1714–1717. https://doi.org/10.1126/science.1115193.
[22] Basu, S.; Lan, X.; Dlugokencky, E. et al. Estimating Emissions of Methane Consistent with Atmospheric Measurements of Methane and $\delta^{13}C$ of Methane. *Atmospheric Chemistry and Physics* **2022**, *22* (23), 15351–15377. https://doi.org/10.5194/acp-22-15351-2022.
[23] Michel, S. E.; Lan, X.; Miller, J. et al. Rapid Shift in Methane Carbon Isotopes Suggests Microbial Emissions Drove Record High Atmospheric Methane Growth in 2020–2022. *Proceedings of the National Academy of Sciences* **2024**, *121* (44), e2411212121. https://doi.org/10.1073/pnas.2411212121.
[24] Zhang, Z.; Poulter, B.; Feldman, A. F. et al. Recent Intensification of Wetland Methane Feedback. *Nature Climate Change* **2023**, *13* (5), 430–433. https://doi.org/10.1038/s41558-023-01629-0.
[25] Feng, L.; Palmer, P. I.; Zhu, S. et al. Tropical Methane Emissions Explain Large Fraction of Recent Changes in Global Atmospheric Methane Growth Rate. *Nature Communications* **2022**, *13* (1), 1378. https://doi.org/10.1038/s41467-022-28989-z.
[26] Peng, S.; Lin, X.; Thompson, R. L. et al. Wetland Emission and Atmospheric Sink Changes Explain Methane Growth in 2020. *Nature* **2022**, *612* (7940), 477–482. https://doi.org/10.1038/s41586-022-05447-w.
[27] Oh, Y., Bruhwiler, L., Lan, X. et al. *CarbonTracker-CH_4 2023*. National Oceanic and Atmospheric Administration (NOAA) Global Monitoring Laboratory, 2023. https://doi.org/10.25925/40JT-QD67.
[28] Miner, K. R.; Turetsky, M. R.; Malina, E. et al. Permafrost Carbon Emissions in a Changing Arctic. *Nature Reviews Earth and Environment* **2022**, *3* (1), 55–67. https://doi.org/10.1038/s43017-021-00230-3.
[29] Riishojgaard, L. P.; Tarasova, O. Reducing Methane Emissions—the "Easy" Way to Keep 1.5 Alive? *Frontiers in Science* **2024**, *2*. https://doi.org/10.3389/fsci.2024.1462219.

Notes:

(1) ppm = the number of molecules of a gas per million (10^6) molecules of dry air

(2) The scientifically correct term to use for the abundance in the atmosphere of compounds such as carbon dioxide and other (greenhouse) gases is dry air mole fraction, expressed as the number of moles of each gas per mole of dry air, often with units of ppm or ppb. However, in the GHG Bulletin, we use the more popular term concentration to avoid possible confusion for the public.

(3) ppb = the number of molecules of a gas per billion (10^9) molecules of dry air

(4) This percentage is calculated as the relative contribution of the mentioned gas(es) to the increase in global radiative forcing caused by all long-lived greenhouse gases since 1750. Radiative forcing is the perturbation to the Earth's energy budget resulting from the increased burdens of greenhouse gases since the pre-industrial (1750) period after allowing stratospheric temperature to quickly adjust. "Effective" radiative forcing also includes fast tropospheric adjustments. Note that the numbers presented here account only for the direct radiative forcing of CH_4 and CO_2, as opposed to the emission-based forcings used in the IPCC AR6 WG1 report, which include estimated indirect forcings due the atmospheric chemistry of CH_4, influencing other atmospheric constituents.

(5) 1 Gt CO_2 = 1 billion (10^9) tonnes of carbon dioxide; 1 Pg = 10^{15} g

(6) ppt = the number of molecules of a gas per trillion (10^{12}) molecules of dry air

Contacts

World Meteorological Organization
Atmospheric Environment Research Division,
Science and Innovation Department, Geneva
Email: gaw@wmo.int
Website: https://community.wmo.int/activity-areas/gaw

World Data Centre for Greenhouse Gases
Japan Meteorological Agency, Tokyo
Email: wdcgg@met.kishou.go.jp
Website: https://gaw.kishou.go.jp

SELECTED GREENHOUSE GAS OBSERVATORIES

Bukit Kototabang (Indonesia)

The Global GAW station Bukit Kototabang is located on the island of Sumatra, roughly 17 km north of the town of Bukittinggi (population: 85 000) and around 120 km north of Padang, the capital of the Province of West Sumatra. Bukit Kototabang (which means "the Hill of the Flying City") is situated in the equatorial zone, on the ridge of a high plateau, at an altitude of 864.5 m above sea level and 40 km off the western coastline. The facilities at the site consist of a large one-storey building, which provides space for offices, meeting rooms and laboratories. On the 300 m^2 flat roof, the air inlet and radiation and meteorological equipment are mounted. The greenhouse gas flask sampling programme started at the station in 2004. The station is reached via a small access road which is closed to the public and is a few kilometres off the westerly main road (moderate traffic) between Padang and Medan. The small access road to the station has allowed farmers to develop the area. The station management has requested support from the West Sumatra authorities to address concerns about altering the surrounding environment.

Bukit Kototabang station
Photo: Meteorology, Climatology, and Geophysical Agency (BMKG)

Location
Country: Indonesia
Latitude: 0.20194 °S
Longitude: 100.31806 °E
Elevation: 864.5 m asl
Time zone: UTC+7
WIGOS ID: 0-20008-0-BKT
GAW trigram: BKT

Baring Head (Aotearoa-New Zealand)

The atmospheric observatory at Baring Head (BHD), a GAW regional station, is operated by the National Institute of Water and Atmospheric Research (NIWA) in Aotearoa-New Zealand. It is located at the top of an 85-metre cliff at the southern tip of the North Island, 10 km to the south-east of Wellington (population: 440 000). The surrounding land has been used for low density livestock farming. The station is frequently exposed to strong southerly winds that have not been in contact with land for at least five days and which are used to monitor the composition of Southern Ocean baseline air. High-precision observations of atmospheric CO_2 at BHD began in 1972. The in situ CO_2 record at the station is the longest in the southern hemisphere and one of the longest in the world. GHG observations at BHD include mole fractions of CO_2, CH_4, CO and N_2O, as well as radio and stable isotopes of CO_2, CH_4 and CO. Emerging techniques are used to measure other constituents, such as radon and carbonyl sulfide. Observations of CO_2 and CH_4 mole fractions are increasingly used for national emissions quantifications using top-down methods that utilise inversion techniques. NIWA collaborates with the National Oceanic and Atmospheric Administration (NOAA) Global Monitoring Division (GMD) and the Scripps Institution of Oceanography (SIO).

Baring Head station
Photo: Dave Allen (NIWA)

Location
Country: New Zealand
Latitude: 41.40819 °S
Longitude: 174.87080 °E
Elevation: 85 m asl
Time zone: UTC+12
WIGOS ID: 0-20008-0-BHD
GAW trigram: BHD

JN 241179